HHS Public Access

Author manuscript

Magn Reson Med. Author manuscript; available in PMC 2014 August 25.

Published in final edited form as:

Magn Reson Med. 2014 February ; 71(2): 783–789. doi:10.1002/mrm.24686.

Application of Direct Virtual Coil to Dynamic Contrast-Enhanced MRI and MR Angiography with Data-Driven Parallel Imaging

Kang Wang, Ph.D.[1], **Philip J. Beatty, Ph.D.**[2,3], **Scott K. Nagle, Ph.D., M.D.**[4,5], **Scott B. Reeder, Ph.D., M.D.**[4,5,6], **James H. Holmes, Ph.D.**[1], **Mahdi S. Rahimi**[6], **Laura C. Bell**[4], **Frank R. Korosec, Ph.D.**[4,5], and **Jean H. Brittain, Ph.D.**[1]

[1]Global Applied Science Laboratory, GE Healthcare, Madison, WI, USA

[2]Physical Sciences, Sunnybrook Research Institute, Toronto, Ontario, Canada

[3]Global Applied Science Laboratory, GE Healthcare, Thornhill, Ontario, Canada

[4]Department of Medical Physics, University of Wisconsin-Madison, Madison, WI, USA

[5]Department of Radiology, University of Wisconsin-Madison, Madison, WI

[6]Department of Biomedical Engineering, University of Wisconsin-Madison, Madison, WI, USA

Abstract

Purpose—To demonstrate the feasibility of Direct Virtual Coil (DVC) in the setting of 4D dynamic imaging used in multiple clinical applications.

Theory and Methods—Three dynamic imaging applications were chosen: pulmonary perfusion, liver perfusion and peripheral MRA, with 18, 11 and 10 subjects respectively. After view-sharing, the *k*-space data were reconstructed twice: once with channel-by-channel (CBC) followed by sum-of-squares coil combination and once with DVC. Images reconstructed using CBC and DVC were compared and scored based on overall image quality by two experienced radiologists using a 5-point scale.

Results—The CBC and DVC showed similar image quality in image domain. Time course measurements also showed good agreement in the temporal domain. CBC and DVC images were scored as *equivalent* for all pulmonary perfusion cases, all liver perfusion cases, and 4 out of the 10 peripheral MRA cases. For the remaining 6 peripheral MRA cases, DVC were scored as *slightly better (not clinically significant)* than the CBC images by Radiologist A and as *equivalent* by Radiologist B.

Conclusion—For dynamic contrast-enhanced MR applications, it is clinically feasible to reduce image reconstruction time while maintaining image quality and time course measurement using the DVC technique.

Corresponding Address: Kang Wang, 1111 Highland Ave., Room 1113, Madison, WI 53705-2275, Phone (608) 263-0066, Kang.Wang@ge.com.

Keywords

parallel imaging; magnetic resonance imaging; direct virtual coil; dynamic imaging; coil combination; channel compression

INTRODUCTION

Dynamic MR applications, such as time-resolved contrast-enhanced MR angiography (MRA) and dynamic contrast enhanced (DCE) MR perfusion imaging, have been used in a wide variety of clinical applications, including peripheral vascular disease (1) and detection and staging of hepatocellular carcinoma (2). Dynamic MRI techniques are frequently combined with high channel count coil arrays, high parallel imaging factors and other *k*-space undersampling techniques to achieve the desired anatomical coverage and spatial-temporal resolution (3–5). During image reconstruction, higher frame rates than would be possible using fully-sampled *k*-space are often generated through interpolation in the temporal direction ("view-sharing") to fill in the missing measurements (referred to as "view-sharing undersampling" hereafter).

After view-sharing algorithms have been applied, images are then reconstructed using conventional parallel imaging (PI) techniques. "Physically-based" techniques (6–8) use explicit knowledge of the coil sensitivity to separate aliased signals and can suffer from artifacts caused by inaccuracies in coil sensitivity calibration (9,10). Alternatively, "data-driven" methods (11–14) use a data-fitting approach to calculate linear combination weights that reconstruct "target" data from neighboring "source" data. Because data-driven methods do not require explicit coil sensitivity maps, they may be advantageous compared to physically-based methods for situations in which accurate coil sensitivity estimation is challenging. For example, the data used for calibration may have been acquired at a different position compared to the dynamic acquisition itself; a common occurrence in applications where multiple breath-holds are used, such as DCE liver perfusion imaging.

Unfortunately, the utility of channel-by-channel data-driven PI reconstruction for dynamic imaging can be limited by computation times and memory burdens that can be prohibitive in the clinical setting on standard reconstruction hardware. This is particularly problematic with high channel count coils, large PI factors and large matrix sizes. Even with multi-thread computation, the reconstruction time for the entire dynamic imaging exam including all the phases can be a significant obstacle. For example, if the entire exam consists of 20 phases and the reconstruction time for each phase is 1 minute longer than the acquisition time of that phase, the overall wait time after the end of acquisition would exceed 20 minutes, which may be clinically unacceptable. This problem rapidly worsens as the user increases the view-sharing undersampling factor for a higher temporal frame rate within the same total scan time, or uses a coil with higher channel count.

Different approaches have been reported to address this challenge. First, physically-based methods have been demonstrated to provide significant computation advantages (6–8), including methods that calculate the coil sensitivity from the accelerated acquisition data (8), and could be considered as alternatives to data-driven methods; however limitations in terms

of the need for accurate coil sensitivities persist (9,10). Second, the synthesis phase of data-driven PI could be accelerated by using image-space point-by-point multiplication instead of *k*-space convolution, described in Ref. (11) as "Method 4"; however, the autocalibrating signals (ACS) lines need to be removed. Third, coil compression methods have been proposed to reduce the number of source channels before the calibration step of the data-driven PI (15–18). Complimentary to reducing source channel count, another technique known as Direct Virtual Coil (DVC) has been proposed to accelerate the reconstruction time by performing coil-combination in *k*-space and merging it with PI synthesis (19), effectively reducing the number of target channels in the synthesis step. In this work, we demonstrate *in vivo* the utility of DVC in three different dynamic contrast-enhanced MR applications: pulmonary perfusion, liver perfusion and peripheral run-off MRA, including clinical evaluation of image quality by experienced radiologists.

THEORY

Brief Overview of DVC

Direct Virtual Coil (DVC) was first proposed by Beatty *et al.* (19), and has been shown for non-time resolved high resolution body imaging (20,21). The central concept of DVC is to perform coil combination earlier in the reconstruction pipeline (i.e. in *k*-space) by using *k*-space coil combination coefficients. Hence, the FFT only needs to be performed once on the virtual coil data set rather than once for each channel, significantly reducing the computation time and memory needed to store images from each individual channel. In addition, the PI un-aliasing coefficients and the DVC coil combination coefficients can be merged, further reducing computational overhead. Thus, the data-driven PI synthesis operation also only needs to be performed once, as opposed to once for each channel in conventional channel-by-channel data-driven PI techniques. These two benefits combine to allow significant acceleration of the computation process and significant reduction of the reconstruction memory needed to store all individual channel images.

DVC with View-Sharing

Figure 1 illustrates the conventional channel-by-channel (CBC) and the proposed DVC view-sharing reconstruction diagrams for 4D dynamic imaging. By reversing the order of FFT and coil combination as well as merging the un-aliasing and coil combination coefficients, the DVC diagram only includes one combined synthesis step and one FFT operation before generating the final image and is therefore significantly faster than the CBC approach.

MATERIALS AND METHODS

Three applications were chosen to demonstrate the feasibility and clinical performance of DVC for dynamic contrast enhanced MRI/MRA: pulmonary perfusion, liver perfusion and peripheral runoff MRA. All protocols were HIPAA-compliant and Institutional Review Board (IRB) approved, and informed consent was obtained from all subjects prior to scanning. All scans were conducted on clinical scanners (3.0T Discovery MR750 or 1.5T

Optima MR450w, GE Healthcare, Waukesha, WI, USA). Study details including subject demographic information and scan parameters for all protocols are listed in Table 1.

For all applications, each raw data set was reconstructed twice: once with CBC followed by sum-of-squares coil combination and once with DVC. Both reconstructions used view sharing. The data-driven PI was performed using ARC (GE Healthcare, Waukesha, WI, USA): proprietary software that employs an indirect calibration procedure (22) to generate unaliasing coefficients in *k*-space together with hybrid-space data synthesis, described by Brau *et al.* (11) as "Method 5". For simplicity and faster reconstruction, both the PI unaliasing calibration and DVC calibration processes for all the reconstructions in this work were performed only once using the pre-contrast image data and used repeatedly thereafter. All reconstructions were performed offline on a Linux machine with 8GB of memory and Intel Core Duo 2.33GHz CPU without multi-threading computation.

Images reconstructed using CBC and DVC were compared in terms of overall image quality and scored using a 5-point Likert scale: image 1 much better (clinically significant); image 1 slightly better (not clinically significant); equivalent; image 2 slightly better (not clinically significant); image 2 much better (clinically significant). For pulmonary perfusion, the peak parenchymal enhancement phase was selected for review by a cardiothoracic radiologist with 8 years of clinical MRI experience (referred to as "Radiologist A"). Images reconstructed using the two methods were evaluated in a randomized order in both coronal and axial orientations. Line profiles and the temporal enhancement waveform of the main pulmonary artery were also compared. For liver perfusion, CBC and DVC axial images at two different phases were selected, randomized and presented to another radiologist with 11 years of clinical MRI experience ("Radiologist B") for comparison. Line profiles and temporal enhancement waveforms were also compared. For peripheral runoff MRA, the best arterial phase was first identified and then a coronal maximum intensity projection (MIP) image and source images were reconstructed using the two methods. These were then randomized and compared by both radiologists.

RESULTS

Figure 2 shows typical results from one of the pulmonary perfusion exams. The CBC images and DVC images are shown in Figure 2(a) for the peak parenchymal enhancement phase in both coronal and axial views. Comparisons of the line profiles on the source images and temporal waveforms of the pulmonary artery are also shown in Figure 2(b) and (c) respectively. Excellent agreement was found in all comparisons, with DVC reconstruction being approximately 6.4× faster than CBC in the parallel imaging reconstruction module (1.5 sec *vs.* 9.7 sec). For all 18 subjects, images reconstructed by the CBC and DVC methods were scored as *equivalent* by Radiologist A. The CBC images demonstrated very slightly increased noise but only appreciable outside the body.

Figure 3 presents the results from a liver perfusion exam in a patient volunteer with hepatocellular carcinoma (HCC), as visualized by the enhancing lesion. CBC and DVC images were compared in the axial plane at two different temporal phases. Line profiles and temporal waveform measurements on an HCC tumor were also compared for CBC and

DVC. Good agreement in terms of image quality, line profiles, and temporal waveform measurements were found in all comparisons, with the DVC reconstruction being approximately 12× faster in the parallel imaging reconstruction module (6.9 sec *vs.* 83 sec). For all 6 subjects, images reconstructed by the CBC and DVC methods were scored as *equivalent* by Radiologist B.

Figure 4 shows typical results from one of the peripheral run-off MRA exams. Arterial-phase coronal MIP images reconstructed using CBC and DVC are shown in the top row. Enlarged and cropped images of the popliteal trifurcation are also shown. Using DVC, images were reconstructed in much shorter reconstruction times than by using CBC images (35.8 sec *vs.* 538 sec, 15× faster). For all 6 subjects in this application, images reconstructed by DVC were scored as *slightly better (not clinically significant)* than the CBC images by Radiologist A because of a slightly lower noise level in DVC outside of the body. Radiologist B scored all cases as *equivalent*, but he observed the same effect and was able to differentiate the two reconstructions consistently.

DISCUSSION

In this work, we have demonstrated the clinical feasibility of the direct virtual coil technique for three different dynamic MR applications. Using the proposed DVC technique, image reconstruction times can be significantly reduced with no compromise in image quality or time course measurement. It can be expected that larger improvement in reconstruction times could be achieved by implementing the DVC algorithm on standard clinical scanner reconstruction engines using multiple processors with proper threading and optimization. Importantly, the improvement in reconstruction times for these studies may also enable the use of even higher spatial-temporal resolution dynamic MR protocols with higher parallel imaging factors.

The improved noise performance in the background with DVC when compared to the CBC sum-of-squares method in regions of low signal observed in this work is believed to be due to the difference in how noise from each channel is added together during coil combination. In regions of low signal, with the CBC sum-of-squares, noise from each channel becomes real-positive valued and hence is added coherently. In contrast, DVC is a complex coil combination algorithm in which the noise from each channel is summed incoherently in a complex-valued form.

The memory requirements of the two techniques differ significantly. The CBC approach typically stores images from each individual channel in memory, which can be very large for some protocols. For example, the peripheral MRA protocol used in this work would require approximately 7.5 GB just to store the 32-channel 512 × 512 × 120 complex floating point data before coil combination; the DVC approach requires only 1/32 of that (approximately 240 MB). Although storing all channel images in memory using the CBC approach is not strictly necessary, this is a common implementation because some phase-sensitive applications, such as IDEAL (23) and 2-point Dixon (24,25), use all individual channel images to estimate a shared B_0 field map.

Another important feature of DVC is that the relative phase of the final coil-combined image across echoes can be preserved throughout the entire reconstruction pipeline, a feature that is essential for any phase-sensitive application such as fat-water separation. An example of a 2-point Dixon fat-water separation technique (24,25) with both CBC and DVC is included in Figure 5, showing the phase difference between the two echoes, and the water and fat images after separation. Good agreement was found between CBC and DVC in terms of the capability of preserving the phase information for water-fat separation. It can be expected that DVC can be extended to other applications that require both dynamic imaging and phase-sensitive processing such as DCE breast MRI (26,27).

Another approach, called channel compression, has recently been proposed (15–18) to address the computation and memory cost for imaging with high channel count coil arrays. In that approach, principal component analysis is used to reduce the number of channels before any PI reconstruction. From this perspective, channel compression is complementary to DVC, in that channel compression can be used to reduce the number of source channels for data-driven PI, and DVC can reduce the number of target channels (17).

CONCLUSION

In this work, we have demonstrated the clinical feasibility of the direct virtual coil (DVC) technique for three dynamic contrast-enhanced MR applications. A significant reduction in image reconstruction time was observed for all three of the applications, and no significant differences in either image quality or temporal waveform measurements were found between the conventional channel-by-channel approach and the DVC approach. The DVC approach has the potential to enable more aggressive protocols for important time-resolved applications such as dynamic contrast enhance perfusion and angiography while maintaining clinically feasible reconstruction times and memory requirements.

ACKNOWLEDGEMENT

Grant sponsor: UW Radiology R&D Committee; NIH; UW School of Medicine and Public Health Wisconsin Partnership Program

Grant numbers: NIH-R01 EB006882 (Korosec); NIH R01 DK083380, R01 DK088925 and RC1 EB010384 (Reeder)

The authors would like to thank Sara Pladziewicz, Jenelle Fuller and Kelli Hellenbrand for recruiting and scanning the subjects.

REFERENCES

1. Zhang H, Maki JH, Prince MR. 3D contrast-enhanced MR angiography. J Magn Reson Imaging. 2007; 25(1):13–25. [PubMed: 17154188]
2. Kanematsu M, Semelka RC, Matsuo M, Kondo H, Enya M, Goshima S, Moriyama N, Hoshi H. Gadolinium-enhanced MR imaging of the liver: optimizing imaging delay for hepatic arterial and portal venous phases--a prospective randomized study in patients with chronic liver damage. Radiology. 2002; 225(2):407–415. [PubMed: 12409573]
3. Wang K, Busse RF, Holmes JH, Beatty PJ, Brittain JH, Francois CJ, Reeder SB, Du J, Korosec FR. Interleaved variable density sampling with a constrained parallel imaging reconstruction for dynamic contrast-enhanced MR angiography. Magn Reson Med. 2011; 66(2):428–436. [PubMed: 21360740]

4. Haider CR, Hu HH, Campeau NG, Huston J 3rd, Riederer SJ. 3D high temporal and spatial resolution contrast-enhanced MR angiography of the whole brain. Magn Reson Med. 2008; 60(3): 749–760. [PubMed: 18727101]

5. Du J. Contrast-enhanced MR angiography using time resolved interleaved projection sampling with three-dimensional cartesian phase and slice encoding (TRIPPS). Magn Reson Med. 2009; 61(4): 918–924. [PubMed: 19195019]

6. Pruessmann KP, Weiger M, Scheidegger MB, Boesiger P. SENSE: sensitivity encoding for fast MRI. Magn Reson Med. 1999; 42(5):952–962. [PubMed: 10542355]

7. Sodickson DK, Manning WJ. Simultaneous acquisition of spatial harmonics (SMASH): fast imaging with radiofrequency coil arrays. Magn Reson Med. 1997; 38(4):591–603. [PubMed: 9324327]

8. Wang J, Kluge T, Nittka M, Jellus V, Kuehn B, Kiefer B. Parallel acquisition techniques with modified SENSE reconstruction mSENSE. Proc of the first Wuerzburg Workshop on Parallel Imaging: Basics and Clinical Applications. 2001:92.

9. Griswold MA, Kannengiesser S, Heidemann RM, Wang J, Jakob PM. Field-of-view limitations in parallel imaging. Magn Reson Med. 2004; 52(5):1118–1126. [PubMed: 15508164]

10. Goldfarb JW. The SENSE ghost: field-of-view restrictions for SENSE imaging. J Magn Reson Imaging. 2004; 20(6):1046–1051. [PubMed: 15558553]

11. Brau AC, Beatty PJ, Skare S, Bammer R. Comparison of reconstruction accuracy and efficiency among autocalibrating data-driven parallel imaging methods. Magn Reson Med. 2008; 59(2):382–395. [PubMed: 18228603]

12. Griswold MA, Jakob PM, Heidemann RM, Nittka M, Jellus V, Wang J, Kiefer B, Haase A. Generalized autocalibrating partially parallel acquisitions (GRAPPA). Magn Reson Med. 2002; 47(6):1202–1210. [PubMed: 12111967]

13. Jakob PM, Griswold MA, Edelman RR, Sodickson DK. AUTO-SMASH: a self-calibrating technique for SMASH imaging. SiMultaneous Acquisition of Spatial Harmonics. Magma. 1998; 7(1):42–54. [PubMed: 9877459]

14. Heidemann RM, Griswold MA, Haase A, Jakob PM. VD-AUTO-SMASH imaging. Magn Reson Med. 2001; 45(6):1066–1074. [PubMed: 11378885]

15. Buehrer M, Pruessmann KP, Boesiger P, Kozerke S. Array compression for MRI with large coil arrays. Magn Reson Med. 2007; 57(6):1131–1139. [PubMed: 17534913]

16. Huang F, Vijayakumar S, Li Y, Hertel S, Duensing GR. A software channel compression technique for faster reconstruction with many channels. Magn Reson Imaging. 2008; 26(1):133–141. [PubMed: 17573223]

17. Huang F, Lin W, Duensing GR, Reykowski A. A hybrid method for more efficient channel-by-channel reconstruction with many channels. Magn Reson Med. 2012; 67(3):835–843. [PubMed: 21713980]

18. Zhang T, Pauly JM, Vasanawala SS, Lustig M. Coil compression for accelerated imaging with Cartesian sampling. Magn Reson Med.

19. Beatty, PJ.; Sun, W.; Brau, AC. Direct Virtual Coil (DVC) Reconstruction for Data- Driven Parallel Imaging. Proc 16th Annual Meeting ISMRM; Toronto, Canada. 2008. p. 8

20. Beatty, PJ.; Cheng, JY.; Shankaranarayanan, A.; Madhuranthakam, A.; Yu, H.; Bayram, E.; Chang, S.; Brittain, JH. Feasibility of Direct Virtual Coil (DVC) Reconstruction for 3-D Imaging. Proc 17th Annual Meeting ISMRM; Hawai'i, USA. 2009. p. 2727

21. Beatty, PJ.; Holmes, JH.; Chang, S.; Bayram, E.; Brittain, JH.; Reeder, SB. Coil-by-Coil vs. Direct Virtual Coil (DVC) Parallel Imaging Reconstruction: An Image Quality Comparison for Contrast-Enhanced Liver Imaging. Proc 18th Annual Meeting ISMRM; Stockholm, Sweden. 2010. p. 2879

22. Beatty, PJ.; Brau, AC.; Chang, S.; Joshi, SM.; Michelich, CR.; Bayram, E.; Nelson, TE.; Herfkens, RJ.; Brittain, JH. A Method for Autocalibrating 2-D Accelerated Volumetric Parallel Imaging with Clinically Practical Reconstruction Times. Proc 15th Annual Meeting ISMRM; Berlin, Germany. 2007. p. 1749

23. Reeder SB, Pineda AR, Wen Z, Shimakawa A, Yu H, Brittain JH, Gold GE, Beaulieu CH, Pelc NJ. Iterative decomposition of water and fat with echo asymmetry and least-squares estimation

(IDEAL): application with fast spin-echo imaging. Magn Reson Med. 2005; 54(3):636–644. [PubMed: 16092103]

24. Ma J. Breath-hold water and fat imaging using a dual-echo two-point Dixon technique with an efficient and robust phase-correction algorithm. Magn Reson Med. 2004; 52(2):415–419. [PubMed: 15282827]
25. Ma J, Slavens Z, Sun W, Bayram E, Estowski L, Hwang KP, Akao J, Vu AT. Linear phase-error correction for improved water and fat separation in dual-echo dixon techniques. Magn Reson Med. 2008; 60(5):1250–1255. [PubMed: 18956418]
26. Kuhl CK, Schild HH, Morakkabati N. Dynamic bilateral contrast-enhanced MR imaging of the breast: trade-off between spatial and temporal resolution. Radiology. 2005; 236(3):789–800. [PubMed: 16118161]
27. Saranathan, M.; Hargreaves, BA.; Moran, CJ.; Daniel, B. Variable-Resolution Dynamic Contrast-Enhanced Breast MRI Acquisition. Proc 19th Annual Meeting ISMRM; Montreal, Canada. 2011. p. 3087

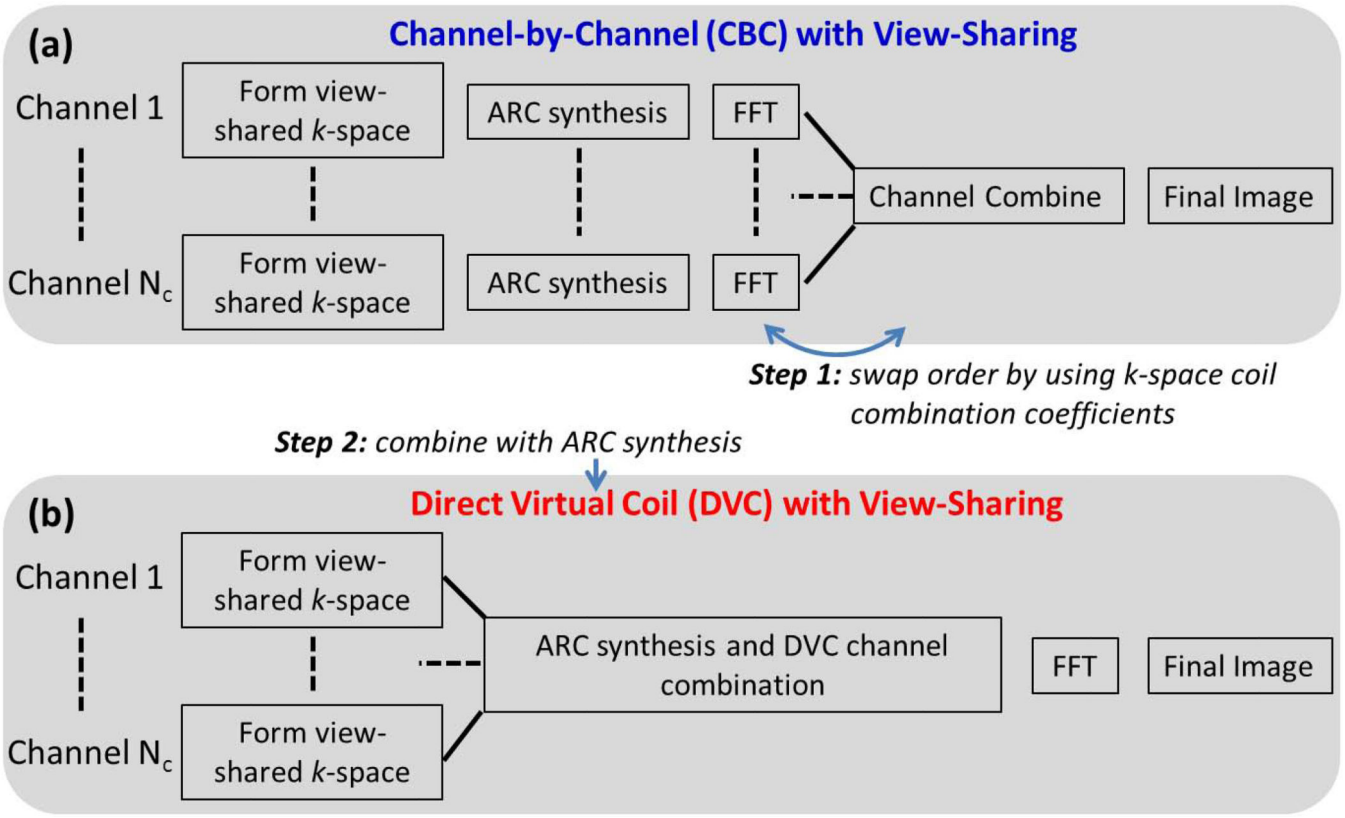

Figure 1.

(a) Reconstruction diagram for view-sharing with the conventional channel-by-channel (CBC) approach. (b) View-sharing reconstruction with the proposed direct virtual coil (DVC) approach. Note that the ARC synthesis and Fast Fourier Transform (FFT) are only performed once in the DVC approach, as opposed to N_c (number of channels) times in the CBC approach, resulting in a significant reduction in reconstruction time and memory requirements.

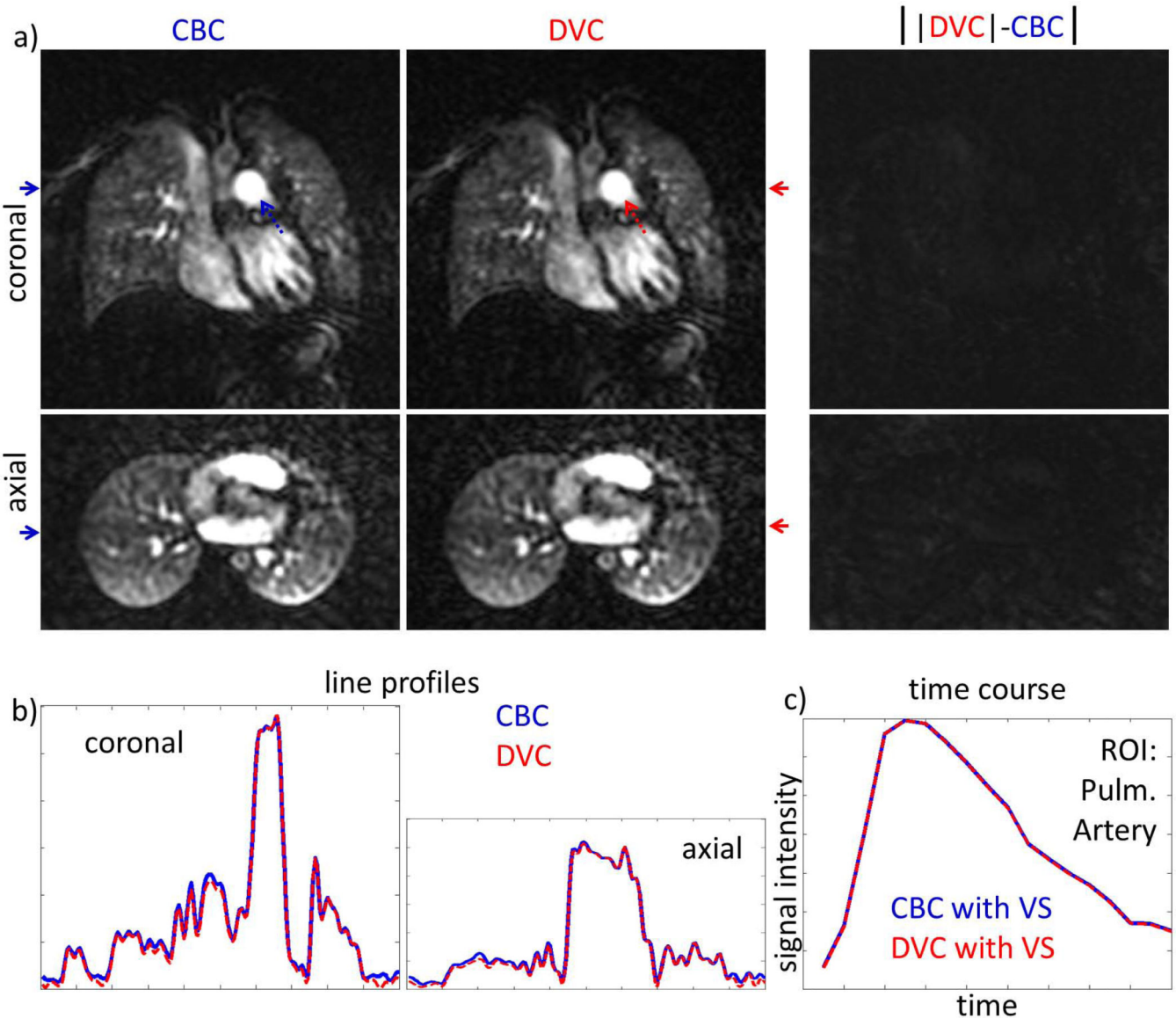

Figure 2.

Pulmonary perfusion results in a normal volunteer, comparing the conventional channel-by-channel (CBC) approach with the proposed direct virtual coil (DVC) approach. (a) Coronal (top row) and axial (bottom row) images at the peak parenchymal enhancement phase. (b) Line profile measurements (position indicated by the arrows in (a)) for both methods. (c) Temporal waveform comparison between the two methods with region of interest (ROI) placed on main pulmonary artery in the coronal plane (dashed arrows). Very good agreement was found between both methods in all comparisons for this application. DVC was about 6.4× faster than CBC for this data set (1.5 sec *vs.* 9.7 sec, 8-channel, R = 2 × 2).

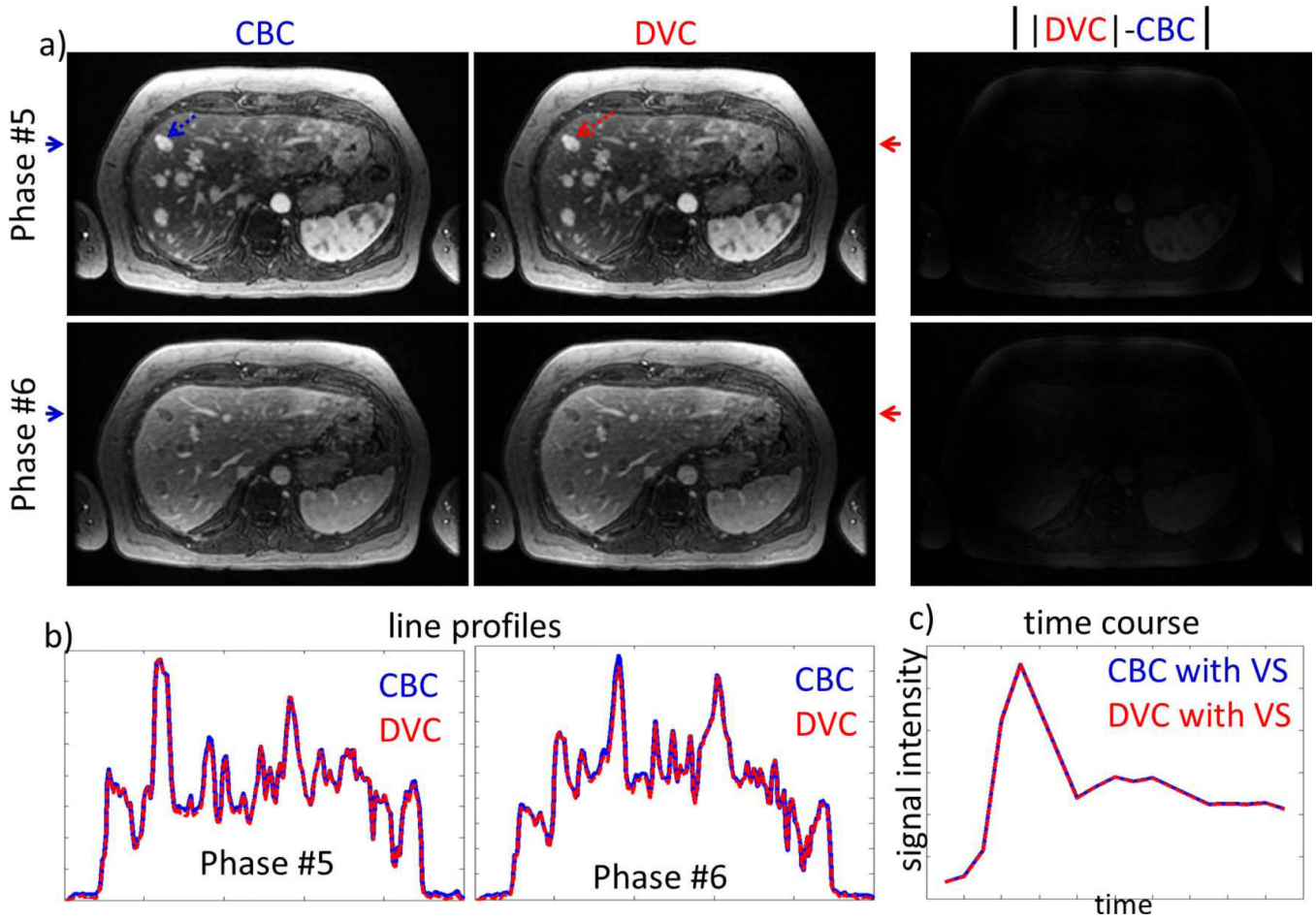

Figure 3.

Liver perfusion results in a patient with metastatic hepatocellular carcinoma, comparing the conventional channel-by-channel (CBC) approach with the proposed direct virtual coil (DVC) approach. (a) Axial images at two phases using the two methods. (b) Line profile measurements (position indicated by the arrows in (a)) for both methods. (c) Temporal waveform comparison between the two methods with ROI placed on an HCC indicated by the dashed arrows in (a). Very good agreement was found between both methods in all measurements. DVC was about 12× faster than CBC for this data set (6.9 sec *vs.* 83 sec, 32-channel, R = 2 × 2).

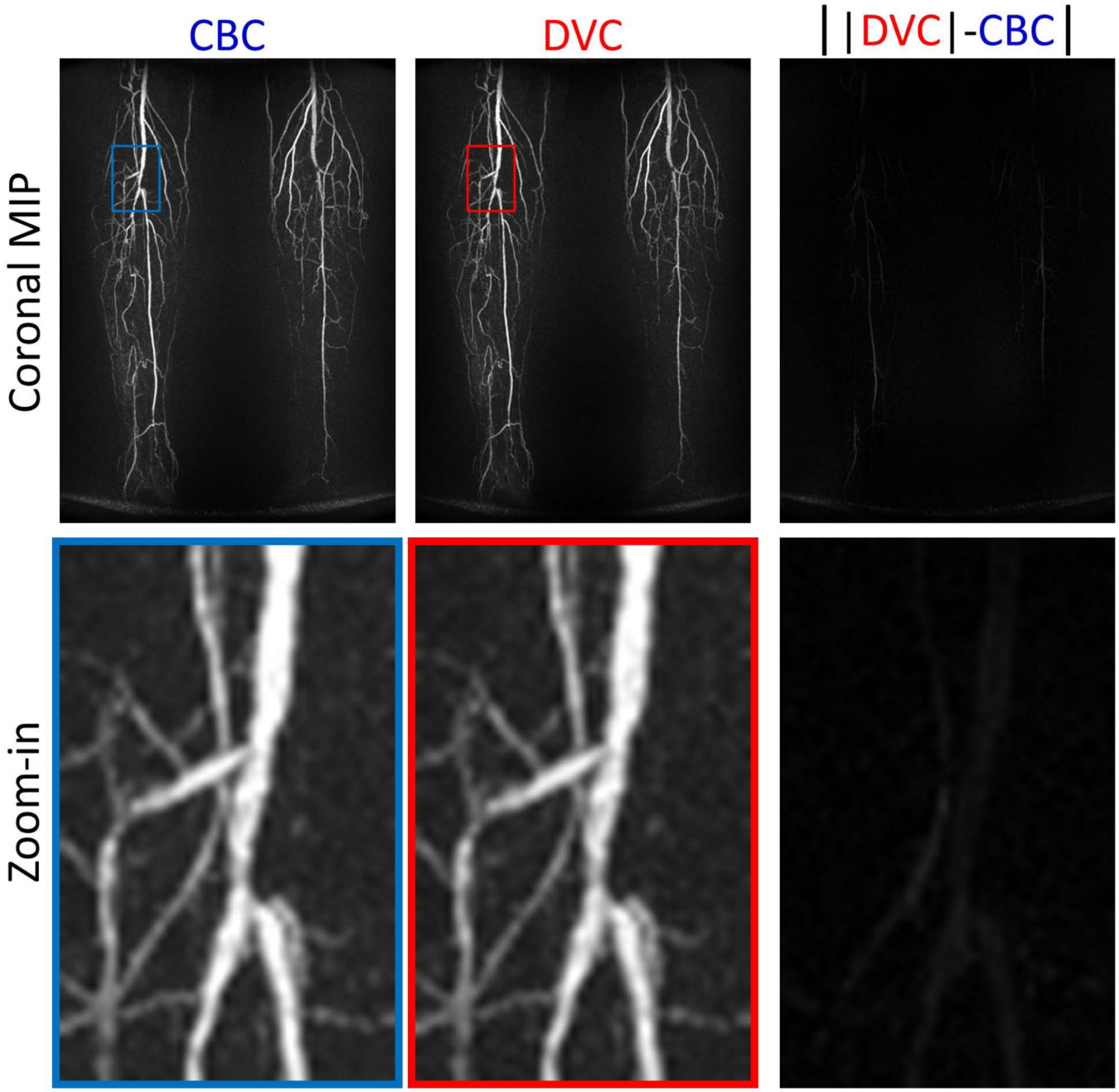

Figure 4.

Results from a peripheral MRA of the calves in a patient with known peripheral vascular disease, showing coronal MIP images (top row) and enlarged images of the peripheral trifurcation, reconstructed using both methods. Very good agreement was found in image quality and detailed vascular structures. If using CBC approach, the reconstruction time for this 24-phases data set would be more than 20 minutes. DVC was approximately 15× faster than CBC for this data set (35.8 sec *vs.* 538 sec, 32-channel, R = 3 × 2).

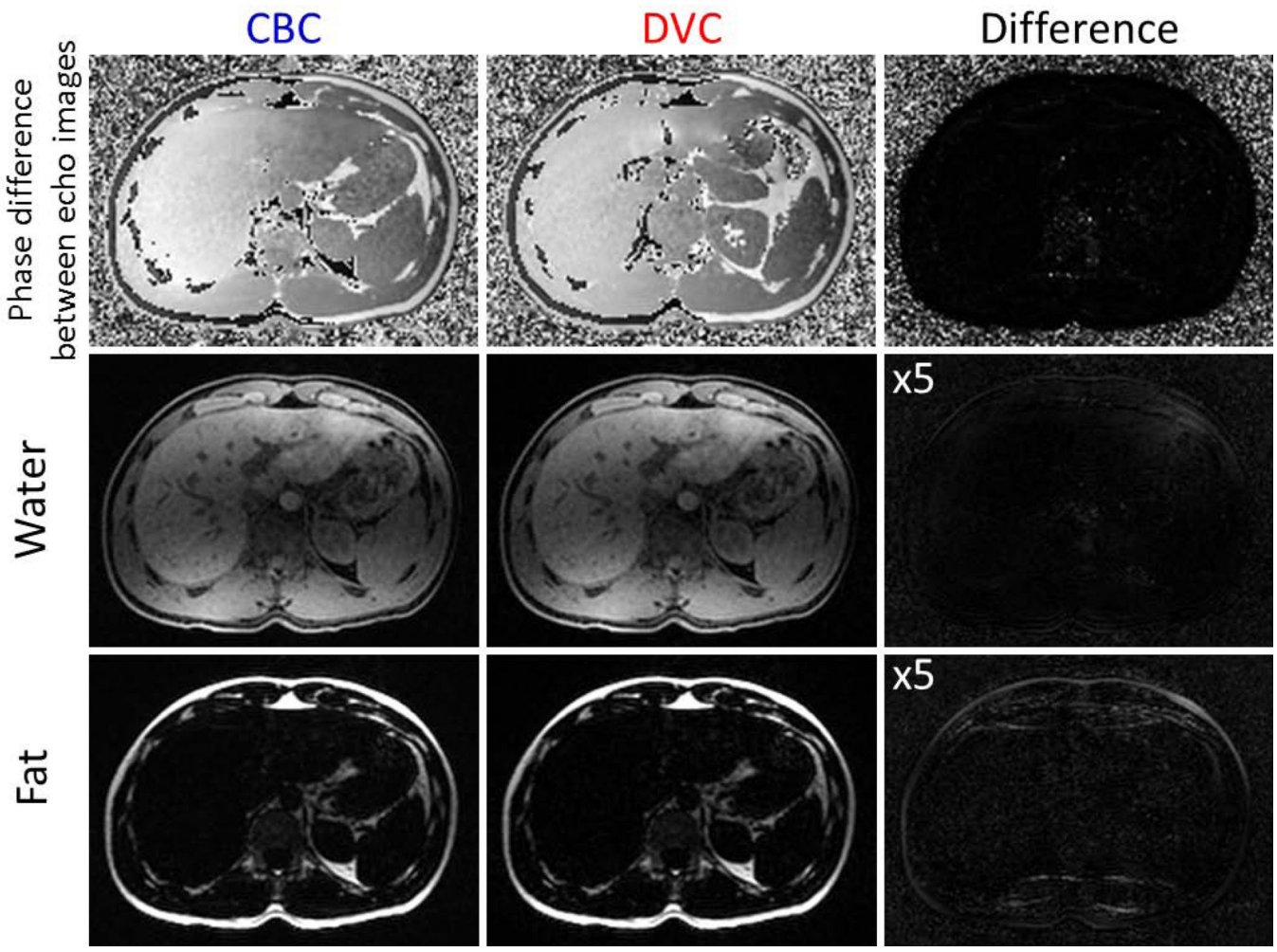

Figure 5.

CBC, DVC and their difference for a 2-point in-phase/out-of-phase Dixon liver imaging. The first row shows the phase difference between the in-phase and out-of-phase echo images. The second and third rows show the water and fat images after separation, for CBC, DVC and their difference multiplied by a factor of 5. 3T, 32-channel torso array with the superior 20 elements selected, FOV = 40 × 32 × 24 cm^3, 2.0 mm isotropic resolution. R = 2 × 2.

Table 1

Imaging parameters for each application

	Pulmonary Perfusion	Liver Perfusion	Peripheral MRA
# of volunteers	18	11	10
Field Strength	1.5 T	3.0 T	3.0 T
Receiver Array	8-channel cardiac	32-channel torso	32-channal torso
FOV	$40 \times 32 \times 40\ cm^3$	$40 \times 32 \times 20\ cm^3$	$48 \times 32 \times 12\ cm^3$
Acquired Matrix	100 × 78 × 100	200 × 162 × 100	480 × 320 × 120
Acquired Spatial Resolution	4.0 mm isotropic	2.0 mm isotropic	1.0 mm isotropic
TR/TE	1.7/0.6 ms	2.6/0.9 ms	5.2/1.9 ms
Parallel Imaging	2 × 2	2 × 2	3 × 2
View-sharing undersampling factor	~3 or ~6	~2.5	~6
Reconstructed Temporal Resolution	1.0 or 0.5 s/frame	4 s/frame	5.4 s/frame
# of phases	18 or 36	15	24